IIETA International Information and Engineering Technology Association
Advancing the World of Information and Engineering

Journal of New Materials for Electrochemical Systems
Vol. 25, No. 4, October 2022, pp.277-285
Journal homepage: http://iieta.org/journals/jnmes

Implantation of Coated Superconducting Materials in the Synchronous Machine for Superconducting Energy Storage

Salah Belkhiri[1*], Zine Ghemari[1], Mohamed Lotfi Khene[2],Fethi Ben Mebarek[2] and Salah Saad[3]

[1] Department of Electrical Engineering, Faculty of technology, University of M'Sila28000, Algeria
[2] Department of Electrical Engineering, Faculty of technology, University of Biskra07000, Algeria
[3] Electromechanical departments, University of Annaba, Algeria

Corresponding Author Email:salah.belkhiri@univ-msila.dz

https://doi.org/10.14447/jnmes.v25i4.a08

Received: May 13-2022
Accepted: October 26-2022

Keywords:
energy storage, torque, second-generation superconducting ribbons, inductor, PMSM.

ABSTRACT

Numerical tools appear to be essential for modeling and designing devices based on superconducting materials. In this article different simulation results are presented, using a computer code based on the finite element method adopted for the resolution of the electromagnetic equations, in the case of an axisymmetric two-dimensional problem, with this code we study the variations of the different electromagnetic quantities. The second generation superconductor has been modeled as an interesting diamagnetic material as inductive pulse sources. The performance in magnetic field resistance, energy storage and thermal stability of the ribbon, known as YBCO, makes it possible to broaden its field of application. Two categories of machines have been proposed and analyzed, the first is classic and the second uses a superconducting ribbon. In addition, a comparative study between the two proposed models is carried out and the results are analyzed and discussed.

1. INTRODUCTION

Research into the heritage of superconductors has been re-launched since this discovery, while industrial applications may be possible. The conventional materials used in the various fields of electrical engineering are generally designed from an adequate assembly of conventional conductors and ferromagnetic materials, the latter have reached their limits of use because of the limitations of their performance, limitations due to heating in resistive materials, and saturation fields in magnetic materials. Superconducting materials seem at first sight to be able to defend against all their harmful drawbacks, thanks to their remarkable properties (zero resistivity, high current density, intense fields, etc.) [1–4]. But things are not quite as simple as we assumed, because superconductors also have their minor drawbacks, in particular the very low critical temperature (around 4.2K°). It is this major drawback which has limited the use of superconductors to particular fields, especially in applications requiring very high magnetic fields produced only by superconducting coils [5–8]. When we consider, to store a certain amount of energy, to use S.M.E.S. (Superconducting Magnetic Energy Storage), we obviously strive to propose a superconducting winding structure with the best performance. The objective is generally set to minimize losses during charging/discharging of the system. It is possible to set other criteria: the improvement of all electromagnetic quantities.

The appearance of superconductors known as: at high critical temperature (HTC) has really approved a new interest in these materials, and encouraged research on the applications of this type of material, in particular for the storage of electrical energy and the production of strong fields. Among the applications of electrical engineering, the most promising seems to be superconducting winding because it brings a new solution to conventional techniques [9].

The conventional electrical machines use copper, iron and permanent magnet as composite material having very high efficiency and very good compactness. These machines are used optimally in order to provide the best possible performance [10–12]. However, today new embedded applications require a gain in compactness and additional performance which is impossible to obtain with technological limitations that we know on conventional machines [13]. The advantages brought by the use of superconductors can be shown from a theoretical point of view by comparing a conventional synchronous motor and a machine of the same topology using superconductors [14]. One of the objectives of research on superconducting materials is related to the development of high-performance superconducting machines. Low critical temperature and high critical temperature superconducting machines are the two generations of known superconducting machines [15–17].

According to their design, they are classified into two categories:

1- Conventional copper machines, their copper windings are replaced by superconducting windings to improve their performance.

2- Machines using superconductors to design new topologies.

Everyone knows that the principle of an electric motor is based on the interaction of the radial magnetic induction (Br) created by the inductor and the tangential field (Ht) produced by the armature and supplied with alternating current, generally three-phase. This interaction generates an electromagnetic torque which is valid if the magnetic field is invariant along the Z axis [18]. Permanent magnet electric

motors currently have the best power-to-weight ratio, also called power-to-power. But this is still insufficient, that's why disruptive technologies are being studied, such as the use of superconducting materials.

Under certain conditions, a superconductor can be used to trap a magnetic field, but also as a field shielding device to guide the magnetic field lines. The material is then used, no longer to channel the magnetic field as one usually did with the ferromagnetic materials, but to deviate it is the diamagnetic effect screen effect to create a new structure of a flux barrier superconducting machine [19–23].

When superconducting materials are used for the armature and the inductor, then the machine is said to be totally superconducting. Partially superconductive machine refers to a structure where only the inductor is superconductive, and the armature is conventional (copper coils). Totally superconducting machines aim to achieve the highest power densities, because the current-carrying capacity of superconductors makes possible a significant increase in the inducing field and the linear current density of the armature. The thickness of the air gap is fixed by the mechanical separation, so it is substantially the same as standard electrical machines. In addition, yields are also increased, due to the elimination of DC losses. However, AC losses in superconducting conductors are still a major problem for the development of these machines today. They are due to the AC currents flowing in the superconductor but also to the variable electromagnetic environment in a machine [24, 25].

Partially superconducting machines have the potential to increase power density over standard electrical machine technologies by reducing or eliminating the use of ferromagnetic materials. The air gap is thicker than a standard or totally superconducting machine, due to the thickness of the thermal insulation between the armature and the inductor and the mechanical air gap. The currents in the superconducting parts are continuous (inductor); moreover the AC magnetic environment can be easily reduced by electromagnetic screens [26, 27]. AC losses are therefore less problematic, which explains why the majority of machines built to date are partially superconducting.

Different machines have been designed and tested by the GREEN laboratory for example: [14, 15, 18]

- Machine with a flux modulation inductor
- Machine with a flux deflection inductor

The particularity of these inductors is the use of combined superconducting wires and massive superconductors. Two superconducting coils are placed on either side of the inductor in the axial direction to create a strong magnetic field and bulk superconductors are used to modulate the magnetic field in the air gap (diamagnetic property).

Other HTc superconducting synchronous machines are produced by several research teams, for example, but not limited to: [17, 28, 30]

-Trapped flux synchronous motor made in Japan where HTc “bulk” magnetized pads are used as permanent magnets. These structures are similar to those with conventional permanent magnets.

-Synchronous reluctance motor made in Russia, where the reluctance is created by stacking HTc “bulks” and ferromagnetic sheets, the salience is due to the ratio of the very low magnetic permeability of the HTc material compared to that of iron. Several rotor combinations have been studied.

-Synchronous motor with hysteresis made in Portugal, the principle of this motor is based on the phenomenon of hysteresis of "bulk" HTc during magnetization by the armature field.

The objective of this study is to implant a second-generation superconducting materials having the particularity of suffering only from low losses (especially in the first thermally activated flux-flow (TAFF) and flux-creep states), when an electric current passes through. We therefore quickly see an advantage concerning their integration in synchronous machines. Two categories exist for YBCO: bulk [29] and thin film (ribbon). For the application of this work, we have chosen to use tapes that are more flexible, more resistant to mechanical stress and therefore easier to roll up than a solid material. The structure presented in this work helps to get a high torque thanks to increase the radial field produced by the inductor which is made from superconducting ribbons. Another phenomenon that was also treated in this study is energy storage. We all know that the classic methods of storing electrical energy, using for the most part an intermediate energy (electrochemical, hydraulic, inertial storage). Magnetic energy storage, or S.M.E.S, uses a short-circuited superconducting coil to store energy in magnetic form. Due to the absence of resistance in the superconducting ribbon, this energy can be stored almost indefinitely.

2. DESCRIPTION OF SECOND GENERATION RIBBON (YBCO)

The device constituting the studied inductor is a conductive type deposited with YBCO, it consists of three main layers (shunt, superconductor and substrate) and several buffer layers. These last layers have a major and important role in machine operation. They also make possible the creation of chemical diffusion barrier preventing the pollution of the superconductor by the elements of the substrate and preventing the oxidation of the latter during the YBCO deposition phase. The simplified architecture adopted for a ribbon of length L rub is described in figure.1.

Second-generation superconducting ribbons have been developed with the aim of getting as close as possible to the native properties of superconductors perfectly textured by epitaxial growth [28, 31]. The architecture of these ribbons is made in the form of a sandwich of three thin layers: the substrate, the superconducting layer and the shunt, (Fig. 1).

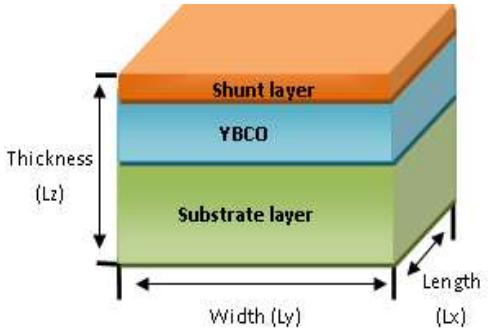

Figure 1. The description of the ribbon model

Each layer has a role in the operation of the winding as developed in the proposed model. The substrate acts as a support, its main function is to dissipate the excessive heat

produced during operation and thus protect the superconducting element. The thickness of the substrate is around 50 µm, the alloys used are Nickel-based (NiCr, Inconel, Hastelloy and Constantan).

They make possible the adaptation of mechanical stresses, resulting from the difference in coefficient of thermal expansion between the superconductor and the substrate, and the difference in lattice parameter between these two materials.

The superconducting layer has a thickness of 1 µm and the shunt has an average thickness of 20 µm, it acts as a thermal and electrical stabilizer. The material used for this layer is silver [32–37].

3. FORMULATIONS

3.1 Putting into equations of the PMSM in the frame (abc)

$$[V] = [R_S][i] + \frac{d[\varphi]}{dt} \tag{1}$$

$[V] = [V_a V_b V_c]^T$: Vector stator voltages.
$[i] = [i_a i_b i_c]^T$: Stator current vector.
$[\varphi] = [\varphi_a \varphi_b \varphi_c]^T$: Stator flux vector.
$[R_s] = \begin{bmatrix} r_s & 0 & 0 \\ 0 & r_s & 0 \\ 0 & 0 & r_s \end{bmatrix}$: Matrix of the equivalent resistance of a stator winding.

The matrix of the inductances, which establishes the linear relations between the fluxes and the currents, is the following:

$$[\varphi] = [\mathrm{L_s}][\mathrm{i_s}] + [\varphi_\mathrm{f}] \tag{2}$$

$[\mathrm{L_s}] = \begin{bmatrix} \mathrm{I_s} & \mathrm{M_s} & \mathrm{M_s} \\ \mathrm{M_s} & \mathrm{I_s} & \mathrm{M_s} \\ \mathrm{M_s} & \mathrm{M_s} & \mathrm{I_s} \end{bmatrix}$: Proper inductance matrix of a stator phase.

$[\varphi_f] = [\varphi_{af} \varphi_{bf} \varphi_{cf}]^T$: Flux vector created by the magnet through the stator winding.

The mechanical equation is written as follows:

$$\mathrm{J}\frac{\mathrm{d}\Omega}{\mathrm{dt}} = \mathrm{C_{em}} - \mathrm{C_r} - \mathrm{C_f} \tag{3}$$

$$\mathrm{C_f} = \mathrm{f_c}\Omega \tag{4}$$

$$\Omega = \frac{\omega_r}{p} \tag{5}$$

With:
$\mathrm{C_r}$: Resistant torque.
$\mathrm{C_{em}}$: Electromagnetic torque.
$\mathrm{C_f}$: Friction torque.
J : Moment of inertia.
$\mathrm{f_c}$: Coefficient of friction.
p :Number of pole pairs
ω_r: Electric rotor speed

3.2 Park transformation

In order to remove the nonlinearity of the system of differential equations, changes of variables is required to reduce the complexity of this system. In three-phase electrical machines, this change of variable consists in transforming the three windings relating to the three phases to orthogonal windings (d, q), rotating at a speed ω. With this transformation, a representation in the three-phase coordinate system (a,b,c) is transformed to a representation in a Cartesian coordinate system of axes (d,q).
From this transformation, the equations are written as follows:

$$\begin{aligned} V_d &= R_s i_d + \frac{d\varphi_d}{dt} - \omega_r \varphi_q \\ V_q &= R_s i_q + \frac{d\varphi_q}{dt} + \omega_r \varphi_d \end{aligned} \tag{6}$$

$$\begin{aligned} \varphi_d &= L_d i_d + \varphi_f \\ \varphi_q &= L_q i_q \end{aligned} \tag{7}$$

By replacing the expressions of the fluxes$\varphi_d$and φ_q in the system

$$\begin{aligned} V_d &= R_s i_d + L_d \frac{di_d}{dt} - \omega_r L_q i_q \\ V_q &= R_s i_q + L_q \frac{di_q}{dt} + \omega_r L_d i_d + \omega_r \varphi_f \end{aligned} \tag{8}$$

The state form is obtained:

$$\begin{aligned} \frac{di_d}{dt} &= \frac{1}{L_d}(V_d - R_s + \omega_r L_q i_q) \\ \frac{di_q}{dt} &= \frac{1}{L_q}(V_q - R_s i_q - \omega_r L_d i_d - \omega_r \varphi_f) \end{aligned} \tag{9}$$

$$\begin{bmatrix} \dot{\mathrm{I}}_\mathrm{d} \\ \dot{\mathrm{I}}_\mathrm{q} \end{bmatrix} = \begin{bmatrix} -\frac{R_s}{L_d} & 0 \\ 0 & -\frac{R_s}{L_q} \end{bmatrix} \begin{bmatrix} \mathrm{I_d} \\ \mathrm{I_q} \end{bmatrix} + \omega_r \begin{bmatrix} 0 & \frac{L_q}{L_d} \\ -\frac{L_d}{L_q} & 0 \end{bmatrix} \begin{bmatrix} \mathrm{I_d} \\ \mathrm{I_q} \end{bmatrix} + \omega_r \begin{bmatrix} 0 \\ -\frac{\varphi_f}{L_q} \end{bmatrix} + \begin{bmatrix} \frac{1}{L_d} & 0 \\ 0 & \frac{1}{L_q} \end{bmatrix} \begin{bmatrix} \mathrm{V_d} \\ \mathrm{V_q} \end{bmatrix} \tag{10}$$

The electromagnetic torque is expressed by the partial derivative of the electromagnetic energy with respect to the geometric angle of rotor rotation expressed below:

$$C_{em} = \frac{dW_e}{d\theta_{geo}} = P\frac{dW_e}{d\theta} \tag{11}$$

According to Park, the expression for the transmitted power is as follows:

$$P(t) = \frac{3}{2}(V_d i_d + V_q i_q) \tag{12}$$

By replacing $V_d V_q$ by their expressions we will have:

$$P(t) = \frac{3}{2}\left[R_s\left(i_d^2 + i_q^2\right) + \left(\frac{d\varphi_d}{dt} i_d + \frac{d\varphi_q}{dt} i_q\right) + \frac{d\theta}{dt}\left(\varphi_d i_q - \varphi_q i_d\right)\right] \tag{13}$$

$\frac{3}{2}R_s\left(i_d^2 + i_q^2\right)$: Represents the power dissipated in Joules losses in the stator windings

$\left(\frac{d\varphi_d}{dt}i_d + \frac{d\varphi_q}{dt}i_q\right)$: Represents the change in magnetic energy stored in the stator windings

$(\varphi_d i_q - \varphi_q i_d)$: Represents the electromagnetic power.

Knowing that:

$$P_e = C_{em}\omega_r \tag{14}$$

He comes:

$$C_{em} = \frac{3}{2}P(\varphi_d i_q - \varphi_q i_d) \tag{15}$$

The expression of the electromagnetic torque as a function of the currents is as follows:

$$C_{em} = \frac{3}{2}P[(L_d - L_q)i_q i_d + i_q \varphi_f] \tag{16}$$

The study of the dynamic behavior of a synchronous electric machine requires a transient magnetic analysis with electromechanical coupling, where the mechanical equation characterizing the movement of the rotor is added to the magnetic or electromagnetic model of the machine.

3.3 Maxwell equations

Macroscopically, Maxwell's equations remain valid to describe the electromagnetic phenomena that occur in a superconductor, they are written.

$$\overrightarrow{\mathrm{Rot}}\vec{\mathrm{E}} = -\frac{\partial \vec{\mathrm{B}}}{\partial \mathrm{t}} \tag{17}$$

$$\mathrm{Div}\vec{\mathrm{B}} = 0 \tag{18}$$

$$\vec{\mathrm{B}} = \overrightarrow{\mathrm{Rot}}\vec{\mathrm{A}} \tag{19}$$

$$\overrightarrow{\mathrm{Rot}}\vec{\mathrm{H}} = \vec{\mathrm{J}}_{\mathrm{t}} \tag{20}$$

For a magnetic medium:

$$\vec{B} = \mu_0 \vec{H} \text{ or } \vec{H} = v\vec{B} \tag{21}$$

For a dielectric medium:

$$\vec{D} = \varepsilon \vec{E} \tag{22}$$

For a conductive medium:

$$\vec{j} = \sigma \vec{E} \tag{23}$$

For a superconducting medium:

In a superconducting medium the relationship between electric field and electric current density is nonlinear, i.e.

$$\vec{\mathrm{J}}_{\mathrm{c}} = \sigma(\vec{E}, \mathrm{T}) \tag{24}$$

The development of the MAXWELL equations governing the electromagnetic behavior of the studied domain leads to the following equations [4,5],where the electromagnetic and thermal coupling is provided by the alternating coupling mode. To model the electromagnetic behavior of the presented study, we have adopted the formulation in magnetic vector potentials A and in electric scalar potential V; this is described by the equation presented below.

$$\begin{aligned} &\nabla \times (\nu \nabla \times \mathrm{A}) - \nabla(\nu \nabla \cdot \mathrm{A}) + \sigma(E,T)\left(\frac{\partial \mathrm{A}}{\partial \mathrm{t}} + \nabla V\right) = \mathrm{J}_{\mathrm{s}} \\ &\nabla . \left\{ -\sigma(E,T)\left(\frac{\partial \mathrm{A}}{\partial \mathrm{t}} + \nabla V\right)\right\} = 0 \end{aligned} \tag{25}$$

υ and σ represent respectively the magnetic reluctivity and the electrical conductivity of the superconductor. Concerning the apparent electrical conductivity of the superconducting material, in its non-dissipative state, it is defined by the ratio of J on E; this ratio is deduced from the characteristic E-J of the superconductor given by the following relation.

$$\sigma_S(E,T) = \frac{J}{E} = \frac{Jc(T)}{Ec}\left(\frac{E}{Ec}\right)^{\frac{1}{n(T)}-1} \tag{26}$$

With: $$Jc(T) = Jc_0 \frac{(1 - \frac{T}{Tc})}{(1 - \frac{T_0}{Tc})} \tag{27}$$

This relation reflects the behavior of the superconductor in a non-dissipative state, to complete the expression of the electrical conductivity of the superconductor in the dissipative regime. An additional term σ_n is added translating the increase in the resistance of the superconductor. Thus, the apparent electrical conductivity of the superconductor is deduced by the relation.

$$\sigma(E,T) = \sigma_s(E,T) + \sigma_n(T) \tag{28}$$

Where $J_C$and E_C respectively represent the density of the critical current and the critical electric field. According to relation (19), the apparent conductivity of the superconductor depends on the electric field E and the temperature T reached within the material. The electric field E will be determined from the resolution of the electromagnetic problem described by the partial differential equation presented by the formulation (17). The temperature will be determined from the resolution of the heat diffusion problem presented by

$$\rho C_p(T)\frac{\partial T}{\partial t} - \nabla.(\kappa(T)\nabla T) = W \tag{29}$$

Where *λ(T), ρ, Cp(T)* are respectively the thermal conductivity in (W / K / m), the density in (Kg / m^3) and the specific heat of the material in (J / K / Kg), W is a power density in (W / m^3), it expresses all the losses generated in the coated superconducting materials given by the following equation:

$$W = E.J \tag{30}$$

We will limit ourselves in this section to a purely "magnetic" study relating to objectives relating to the distribution of the energy stored in the inductor. Compared to other types of storage, magnetic energy storage does not require reconverting the energy, directly accessible in electrical form, and allows flexible and almost infinite cyclability. So it has very high storage efficiency. The magnetic energy stored in the system is then obtained as the half-product of the equivalent total inductance of the system times the square of the current flowing in each strip.

Energy and power are expressed as in equations (31) and (32)

$$E = 1/2\ LI^2 = 1/2 \iiint B\ H\ dxdydz \quad (31)$$

$$P = dE/dt \quad (32)$$

Where 'I' is the current through the coil and 'L' is the superconducting coil inductance, the SMES stores the energy as circulating current, and provide the energy with instantaneous response.

4. PRESENTATION OF SIMULATION PARAMETERS

This part sets up the choices made on the materials and properties that will be used for the simulations that will follow. The various parameters used in the simulation are presented in the following three tables:

Table 1. Simulation parameters for the superconducting material YBCO and Copper

Symbol	Amount	Value (YBCO)	Value (Copper)
γ	Volumic mass	5.4 g/cm^3	8,96 g/cm^3
C_p	Specific heat	150 J/(Kg.K)	385 J/(Kg.K)
λ	Thermal conductivity	5 W/(m.K)	380 W/(m.K)
h	Cryogenic fluid convection coefficient	400 W/(m^2.K)	-
Tc	Critical temperature	93 K	-
Ec	Critical electric field	1 µV/cm	-
J_{c0}	Critical current density at 77 K under zero field	500 A/mm^2	-
n_0	Exponent n at 77 K under zero field	20	-

Table 2. Parameters of the studied machine

Amount	Value
Resistance of a winding	R = 1.4 Ω
direct inductance	Ld = 6.6 mH
quadratic inductance	Lq = 5.8 mH
Number of poles	P = 8
Friction	F= 0.0003881
Number of teeth/pole	6
Magnet	NdFeB
Lamination type	M270-35A
Remanent flux density (NdFeB)	1.2 T
Energy density (NdFeB)	380 (KJ/m^3)
coercive field (NdFeB)	860 10^3 (A/m)

Table 3. Simulation parameters for the materials that make up the ribbon

Symbol	Amount	Value	
		Silver	Hastelloy C-276
γ	Volumic mass	10500 Kg/m^3	8890 Kg/m^3
C_p	Specific heat	235 J/(Kg.K)	427 J/(Kg.K)
λ	Thermal conductivity	429 W/(m.K)	7 W/(m.K)
σ	Electrical conductivity	61,6 ×10^6 S/m	77 ×10^4 S/m

In this phase, we will focus on the study of the temporary evolution of different electromagnetic quantities within two proposed machines. The proposed inductor is composed from two coaxial superconducting ribbon solenoids and a screen. The two solenoids are fed by a direct current having two different directions, and generate a magnetic field as shown in Figure 2.

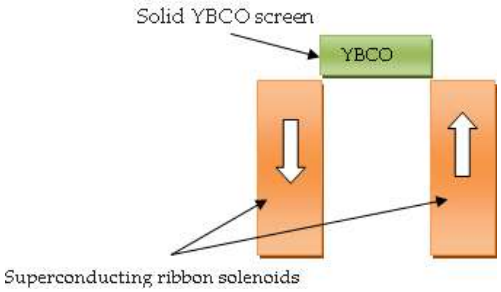

Figure 2. Structure of the studied inductor

Table 4. Geometric parameters of the studied inductor

Amount	Value
Thickness of solid YBCO	15 mm
Width of solid YBCO	40 mm
Length of the solenoid	60 mm
Solenoids outer radius	65 mm
Solenoids inner radius	54 mm

5. NUMERICAL RESULTS AND DISCUSSION

This section is devoted to the different simulation results obtained, the study is focused on the variations of the different electromagnetic parameters, namely (current, speed, magnetic flux density, electromagnetic torque, etc.) of the two machines (conventional and superconducting).Our code, based on the finite element method adopted for the resolution of the equation describing the behavior of the ribbon implanted in the inductor of the machine in the case of an axisymmetric two-dimensional problem.A comparative study between the two proposed models is conducted.

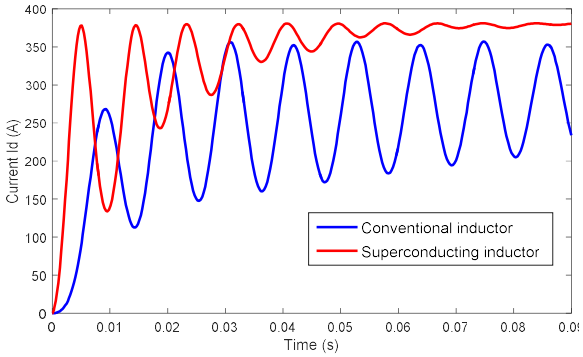

Figure 3. Variation of current Id as a function of time

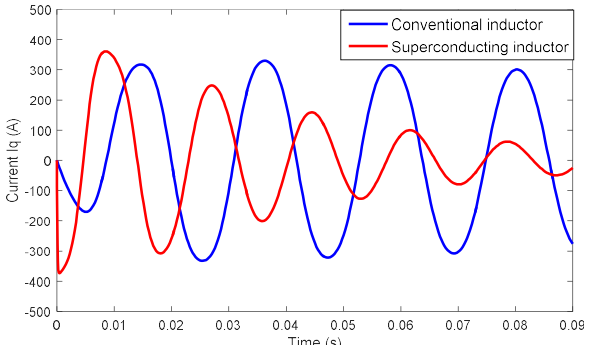

Figure 4. Variation of current Iq as a function of time

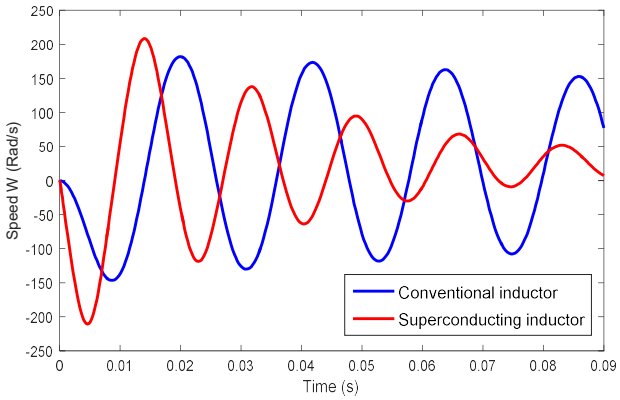

Figure 5. Variation of speed W as a function of time

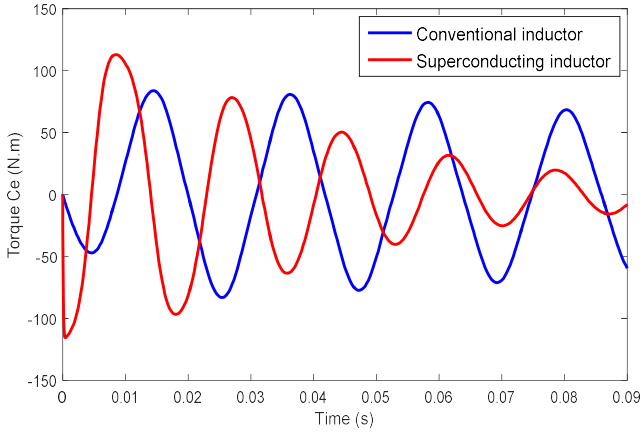

Figure 6. Torque variation Ce as a function of time

The figures above (3-6) represent the development of some fundamental variables of two studied machines, namely the direct and quadrature components of the current and the speed. In no-load operation, in the Permanent Magnet Synchronous Machine (PMSM), there is an excessive inrush of current when the motor is powered up in transient state which stabilizes to give rise to a sinusoidal shape of constant amplitude.

There is also an increase in the amplitude of stator currents.According to the electromagnetic torque equation, its shape is derived from the shape of the current in quadrature Iq, it is found that the effect of the salience slightly influences the main torque.

From these results, the speed oscillates in the transient regime until it stabilizes in the steady state at a fixed value. The speed up time is determined by the total inertia around the rotating shaft, the motor not being loaded, the speed reached is equal to the synchronism speed.

Now, regarding the superconducting machine, from the presented results where a comparison has been conducted in terms of current (Id, Iq), rotational speed (ω) andthe torque (C_e),we clearly see a significant difference between the results of the characteristics of two machines in particular the reduction of transient oscillations and these quantities stabilize more quickly before even the end of the transient regime.

It is also noted that these simulation results have shown the interest and the efficiency of the superconducting materials introduced in the design of an electric machine. These significantly improve thermal stresses during the operating process by reducing joule losses. Thus they can considerably extend the life of superconducting materials.

Fig. 7 presents and compares important characteristics of these two inductors, it is observed that the position of the rotor starts from a low value and increases as a function of time. It is also observed that the superconducting inductor machine has a superior position compared to the conventional machine.

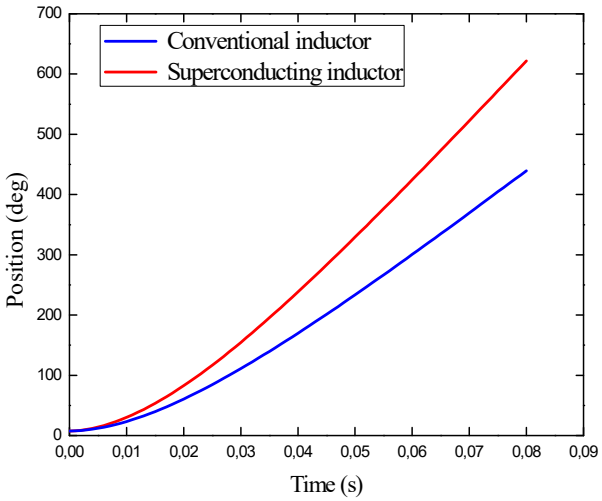

Figure 7. Rotor position as a function of time

In figure 8, the rotational speed is presented as a function of time for the two studied cases. From these simulation results, it can be observed that the curves follow the same trajectory. Nevertheless, the speed values obtained by the superconducting inductor are much higher than those obtained in the case of a conventional inductor. It can be noted that this speed reaches a maximum value of 6950.54deg/s for a conventional machine and a value of 9998.84deg/s for a superconducting machine.

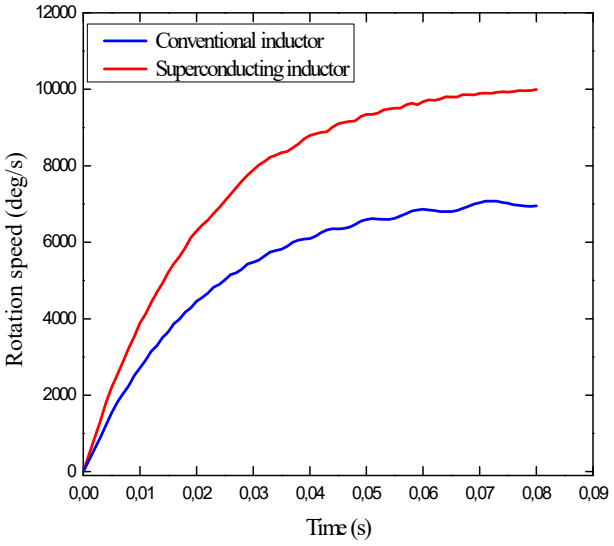

Figure 8. Rotation speed (rotor)as a function of time

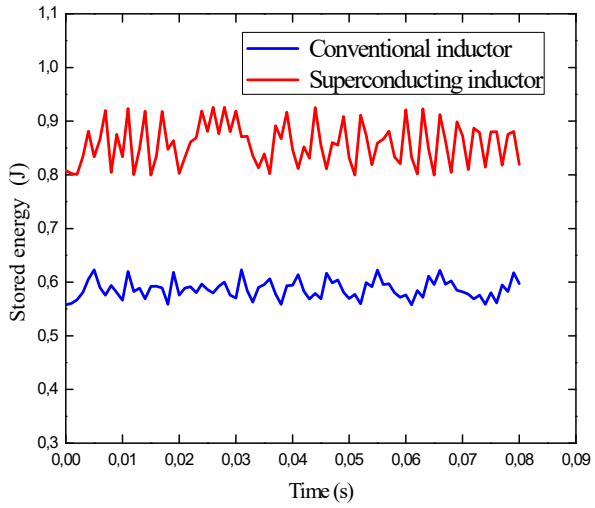

Figure 9. Stored energy as a function of time

Figure 9 shows the stored energy as a function of time, it is known that in order to let the current flow in the inductor, it is necessary to supply energy to this conductor. This energy subsequently is stored by the magnetic field of the inductor and recoverable once the current is switched off.

Therefore starting from the expression relating energy and power, it appears according to the results presented in figure 9, that when we consider a current passing through the superconducting inductor this stored energy reaches its maximum at 0.94 J, meanwhile in a copper inductor inductance at 0.62 J. This is explained by the fact of the important characteristics. Indeed the storage and conservation of electrical energy poses serious problems, as for electrochemical methods, their inability to quickly exchange energy with external circuits. The use of conventional electromagnetic devices for the storage of electrical energy hardly leads to better performance even with the use of good conductors, but unlike conventional storage, electromagnetic storage by second-generation superconducting coils allows energy exchanges. fast energy with electricity use network.

brought by the introduction of superconducting materials which behave like perfect conductors in a diamagnetic medium. The calculation code gives the inductance matrix of the simulated coil system. The inductances obtained are those of the simulated coil systems but where the coils are considered to be made of a single conductor. Each coil being in fact made up of thousands of turns (their number is obtained by dividing the total section of the winding by the section S of the superconducting tape), it is advisable to weight each term of the inductance matrix by the square of the number of turns for the proper inductances and by the product of the numbers of turns of the coils considered for the mutual inductances.

6. CONCLUSIONS

In this paper, an inductor design strategy to improve the electromagnetic properties in the permanent magnet synchronous machine using second-generation superconducting material was proposed. The efficiency of the proposed model was tested using our calculation code under MATLAB.

The results obtained for the two models are compared for a time step of 0.09 s. This choice can be explained by the large number of mesh elements presented in the field discretized with the FEM. This would significantly increase the computation time. Superconducting machines are known to represent an encouraging means of making superconductivity commercially operational in real power systems. The rapid development of type II superconducting materials is linked to the improvement of their performance.

The results obtained showed that the objectives of the present contribution are achieved and indeed, the electromagnetic characteristics such as torque, rotational speed and stored energy are improved both in steady state and in transient state. These results demonstrate that the use of thin films has considerably improved the electromagnetic behavior of the superconducting inductor by the superconducting coils which must be supported by materials with excellent mechanical properties and poor thermal properties.

The study presented in this work made possible the illustration of the superconducting inductor principle towards the optimization on cycle of the synchronous machines with magnets by an original approach entirely digital.

The future trends will be mainly dedicated to the sizing and optimization of the superconducting inductor taking into account the magnetic losses that may occur during machine operation. It is a question of establishing a model of magnetic losses for the latter.

ACKNOWLEDGMENT

The authors would like to thank Editors and reviewers for their pertinent comments and suggestions to improve our work. The authors thank the General Directorate of Scientific Research and Technological Development (DGRSDT).

REFERENCES

[1] Demetriou, P.,Asprou, M.,Quiros-Tortos,J.,Kyriakides, E. (2015).Dynamic IEEE Test Systems for Transient Analysis. IEEE Systems Journal, Vol. PP, no.99, pp.1-10.

[2] Belkhiri,S.(2019).Modeling a superconducting fault current limiter inserted in a nine-bus electrical network.

AMSE. IIETA Journal, Modelling. A, Vol. 92, nº. 2-4, pp. 37-42.

[3] Belkhiri, S.,Bouroubi,M.,Harrabi, A. (2020).Improvement of the Transient Stability of a 14-bus Network Using a Superconducting Fault-Current Limiter SFCL. Advanced Electromagnetics. Vol. 9, no.2, pp. 75-83.

[4] Belkhiri, S.,Alloui, L.,Mebarek, F. B. (2019).The influence of Geometrical Properties of Bulk Superconductors on Limiting Fault Current in an Electrical Network. Advanced Electromagnetics. Vol. 8, no.4, pp. 136-142.

[5] Belkhiri, S. (2018).Study of the implantation of superconducting materials in electrical networks. Doctoral thesis, University of Biskra, Algeria.

[6] Mercy, R. K.,Maheswara, U. R. M. (2017).Transient stability improvement of microgrids by using Resistive type SFCL and series active power filters. Journal EJEE, Vol. 19, no.3-4, pp. 181-195.

[7] Vishwakarma, S. (2018). Transient stability analysis of two area power system using unified power flow controller. Journal of Advances in Modelling and Analysis. C 73 (4) 123-127.

[8] Boyang, S. A.,Yu, C. B.,Chuanyue, L. c.,Sheng, W. C.,Xiaoyuan, C. B. (2021). Superconducting fault current limiter (SFCL): Experiment and the simulation from finite-element method (FEM) to power/energy system software," Energy 234 121251, https://doi.org/10.1016/j.energy.2021.121251

[9] Belkhiri, S.,Ghemari, Z. (2022). Comparative Study of Solid and Thin-Layers Superconducting Fault Current Limiters SFCL for Electrical Network Transient Stability Improvement.Journal of Superconductivity and Novel Magnetism.Vol. 35, Nº 3, pp.679-688. https://doi.org/10.1007/s10948-021-06128-x

[10] Dolisy, B. (2015).Study of a superconducting axial flow motor with integrated superconducting magnetic transmission. Doctoral thesis, University of Lorraine.

[11] Dolisy, B.,Lubin, T.,Mezani, S. and al. (2014).Three-Dimensional Analytical Model for an Axial-Field Magnetic Coupling. Progress In Electromagnetics Research M.Vol. 35, p. 173-182.

[12] Dolisy, B.,Mezani, S.,Lubin, T. and al, (2014).3D analytical modeling of a superconducting axial flux coupling. In: Young Researchers in Electrical Engineering (JCGE'14), p. 1-10.

[13] Bertinelli, F.,Comel, S.,Harlet, P.,Peiro, G.,Russo, A. andTaquet, A. (2006).Production of Low-Carbon Magnetic Steel for the LHC Superconducting Dipole and Quadrupole Magnets. IEEE Transactions on Applied Superconductivity, Vol. 16, no. 2, p. 1777-1781.

[14] Masson, P.,Levêque, Netter, J. D.,Rezzoug, A. (2003).Experimental study of a new kind of superconducting inductor. IEEE Trans. Appl. Supercond., 13, 2239–2242. doi:10.1109/tasc.2003.813055.

[15] Ailam, E. H. (2006).Synchronous machine with superconducting studs: Study and production.Doctoral thesis, University of Henri Poincaré, Nancy-I.

[16] Ailam, E. H.,Netter, D.,Leveque, J.,Douine, B.,Masson, P. J. and Rezzoug, A. (2007). Design and Testing of a Superconducting Rotating Machine. IEEE Transactions on Applied Superconductivity, Vol. 17, no. 1, pp. 27- 33.

[17] Alhasan, R. (2015). Study and production of a new structure for a superconducting synchronous motor," Doctoral thesis, University of Lorraine.

[18] Matsuzaki,H. et al.(2007). HTS Bulk Pole-Field Magnets Motor With a Multiple Rotor Cooled by Liquid Nitrogen. IEEE Transactions on Applied Superconductivity, Vol. 17, no. 2, p. 1553-1556.

[19] Leclerc, J.,Douine, K. B.,Leveque, J. (2012).Enhancement of the E(J,B) power law characterization for superconducting wires from electrical measurements on a coil. IEEE Transaction on Applied Superconductivity, Vol.22, Issue 3.

[20] Leveque, J.,Netter, D. and Rezzoug, A. Patent: Electric motor comprising an inductor with a superconducting element integrated between windings. No. FR20070059915 20071218.

[21] Alhasan, R.,Lubin, T.,Adilov, Z.M. Leveque, J. (2016).A new kind of superconducting machine. IEEE Transaction on Applied Superconductivity, Vol.26, Issue 3.

[22] Alhasan, R.,Lubin, T.,Douine, B.,Adilov Z. M. and Leveque, J. (2016). Test of an Original Superconducting Synchronous Machine Based on Magnetic Shielding. IEEE Transactions on Applied Superconductivity, Vol. 26, no. 4, pp. 1-5.

[23] Alhasan, R.,Lubin, T. and Leveque, J. (2014).Study and test of a new superconducting inductor structure for a synchronous machine. Electrical Sciences and Technologies in Maghreb (CISTEM), International Conference on. IEEE, Tunis, pp. 1-7.

[24] Malé, G. (2012).Study of a superconducting inductor structure with magnetic field modulation.Doctoral thesis, University of Lorraine.

[25] Casali and al. (2015).Two-Dimensional Anisotropic Model of YBCO Coated Conductors. IEEE Trans. Appl. Supercond, Vol. 25, no. 1, pp. 6600112.

[26] Bernstein, P.,Colson, L.,Dupont, L. and Noudem, J. (2017).Investigation of the levitation force of field-cooled YBCO and MgB2 disks as functions of temperature. Supercond. Sci. Technol. 30,065007.

[27] Bernstein, P. et al. (2018).A new approach to the current distribution in field cooled superconductor's disks. Supercond. Sci. Technol. 31, 015008.

[28] Ainslie, M. D.,Fujishiro, H.,Ujiie, T.,Zou, J. A.,Dennis, R.,Shi, Y-H. and Cardwell, D. A. (2014).Modelling and comparison of trapped fields in (RE)BCO bulk superconductors for activation using pulsed field magnetization. Supercond. Sci. Technol. 27,065008.

[29] Douma, B. C.,Abderezzak, B.,Ailam, E.,Felseghi, R-A Filote, C.,Dumitrescu,C. and Raboaca, M. S. (2021). Design Development and Analysis of a PartiallySuperconducting Axial Flux Motor Using YBCO Bulks. Materials, 14, 4295. https://doi.org/10.3390/ma14154295

[30] Kovalev, L. (2003). High output power electric motors with bulk HTS elements. Physica C: Superconductivity, Vol. 386, p. 419-423.

[31] Inácio, D.,Inácio, S., Pina, J., Gonçalves, A., Neves, M. V. et Rodrigues, A. L. (2008).Numerical and experimental comparison of electromechanical properties and efficiency of HTS and ferromagnetic hysteresis motors. Journal of Physics: Conference Series, Vol. 97, p. 012218.

[32] Ainslie, M. D.,Fujishiro, H.,Mochizuki, H.,Takahashi, K.,Shi,Y-H.,Namburi, D. K.,Zou, J., Zhou, D.,Dennis A. R. and Cardwell, D. A. (2016).Enhanced trapped field performance of bulk high temperature superconductors using split coil, pulsed field magnetization with an iron yoke. Supercond. Sci. Technol. 29,074003.

[33] Dupont, L. (2018).Development of a magnetic field device based on superconducting cryo-magnets. Doctoral thesis, University of Normandy.

[34] Colle, A. (2020).Study of a superconductive axial flow machine for an aeronautical application.Doctoral thesis, University of Lorraine.

[35] Elbaa, M. (2020).Characterization and modeling of superconducting materials at high critical temperatures.Doctoral thesis, University of Lorraine, University of Laghouat, Algeria.

[36] Bendali, S. (2012).Sizing of an HTc superconducting motor.Doctoral thesis, University of Lorraine.